Deep-hole interferences in photon-induced Auger emission from solids

S. Abraham-Ibrahim,* B. Caroli,† C. Caroli, and B. Roulet
Groupe de Physique des Solides de l'Ecole Normale Supérieure, associé au Centre National de la Recherche Scientifique, Université Paris VII, 2 Place Jussieu, 75221 Paris—Cedex 05, France
(Received 30 June 1977)

A complete formalism for the description of photon-induced Auger emission is set up, which includes explicitly the process of creation of the deep hole. It is shown that the phase coherence between the holes may induce contributions to the Auger current due to interferences between Auger processes involving the different degenerate deep hole states. It is shown that one must distinguish two types of interferences: intra-atomic ones, between degenerate hole states on the same atomic site, which are practically not affected by lifetime effects; extra-atomic ones, which only occur if at least one of the intermediate states of the Auger process belongs to a wide band. Their space range is limited, by lifetime and mean-free-path effects, to a few atomic distances in light materials. Differences between photon- and electron-induced Auger emission and possible experimental checks of interference effects are discussed qualitatively.

I. INTRODUCTION

Until recently, the Auger emission of solids has been used mostly as a tool for chemical analysis of surface compositions. The new experimental developments now permit not only identification of Auger lines and measurement of the corresponding total current but also analysis of the energy distribution of the Auger current (EDC) and its angular distribution.

One can hope therefore to use the Auger effect to obtain information about the electronic properties of solids in the surface region—in particular by studying Auger transitions involving at least one valence electron. In order to perform this program, one of course needs a theory as complete and systematic as possible, which should be, in particular, able to include, if necessary, many-body effects.

Up to now, Auger EDC's are always calculated[1] with the implicit assumption that the Auger process is independent of the deep-hole creation process: it is stated that the total emission probability is the *product* of the hole creation probability and the Auger probability itself. This entails that, in this model, the line shape and the angular distribution of the current are independent of the hole-creation process.

However, it is by no means obvious that such a decoupling is always justified. It is clear, for example, that when many-body effects are present, they can provide a coupling between the two "steps." This has been shown explicitly in the case of threshold singularities in x-ray emision[2] and in the x-ray resonant Raman scattering of metals[3] (which both involve, as does the Auger effect, a deep-hole creation followed by an emission process).

On the other hand, even if many-body effects are neglected, one should still take into account the physical fact that deep holes are excited coherently by the incident electron or photon field. This phase coherence must give rise to interference effects, which do not appear in the usual theory, since it excludes any correlation between hole creation and emission process.

In this article, we concentrate on the study of these interference effects in the simplest possible model, where many-body effects are assumed phenomenologically to give rise only to finite lifetimes for the various levels involved. Moreover, we only study in detail the case where the deep hole is created by absorption of x-ray photons (creation by electron bombardment is discussed only qualitatively in Sec. V).

In Sec. II, we derive the general formal expression of the energy and angular distribution of the Auger current and show explicitly, in the independent-electron approximation, how interference effects between deep-hole states appear. In Sec. III, completely neglecting many-body effects, we classify interferences into intra- and extra-atomic ones, and discuss in detail some simple examples. In Sec. IV, we include lifetimes and study their effect on the two types of interferences. Finally, we discuss briefly in Sec. V the difference between electron- and photon-induced Auger effect, and the possible experimental checks of the importance of interferences.

II. GENERAL EXPRESSION OF THE AUGER CURRENT

Let us consider a semi-infinite solid at zero temperature, in the presence of a monochromatic electromagnetic field of frequency Ω, described by the vector potential

$$\vec{A}(\vec{r},t)=\vec{a}(\vec{r})\cos\Omega t\ , \tag{1}$$

which decays inside the solid on a penetration depth δ along the direction $\hat{x}$ normal to the solid surface ($x=0$).

As discussed in Refs. (4 and 5), the total dc electron current emitted at infinity in the vacuum ($x \to +\infty$) along the direction of observation $\hat{R}$ and in the energy range $(\omega, \omega+d\omega)$ is (for the two spin directions) $j(\hat{R},\omega)\,d\omega$, where

$$j(\hat{R},\omega)=\frac{e\hbar}{2\pi m}\lim_{\substack{\vec{R}'\to\vec{R}\\ R\to\infty}}\left(\frac{\partial}{\partial R'}-\frac{\partial}{\partial R}\right)\mathcal{G}_{\omega}^{(2)+-}(\vec{R},\vec{R}'), \qquad (2)$$

where $\vec{R}=\hat{R}R$ and $\hat{R}$ the unit vector pointing out of the solid along the direction of observation,

$$\mathcal{G}_{\omega}^{(2)+-}(\vec{R},\vec{R}') = \int dt\,dt'\,\mathcal{G}^{(2)+-}(\vec{R}t;\vec{R}'t')e^{-i\omega(t-t')}, \qquad (3)$$

$\mathcal{G}^{(2)+-}$ is the term of second order in $\vec{A}$ in the electron-occupation propagator of the complete (solid–electromagnetic-field) system.

$$\mathcal{G}^{+-}(\vec{R}t;\vec{R}'t')=i\langle\psi^{\dagger}(\vec{R}'t')\psi(\vec{R}t)\rangle, \qquad (4)$$

$\psi^{\dagger}$ and ψ being the electron creation and destruction operators.

Expression (2) gives the angular and energy distribution (AEDC) of the total photoemission current; that is, it contains the contributions of all possible processes induced by photon absorption and giving rise to subsequent electron emission.

Among these, we want to select here what constitutes the Auger current, namely, processes in which, due to Coulomb interaction, the deep hole (h) created by optical absorption is filled by an electron from a higher-energy state (p), the excess energy thus released being used to excite another electron from a filled state (n) to an empty one $\phi_>$ of energy ω (Fig. 1). Energy conservation imposes

$$\omega=\epsilon_n+\epsilon_p-\epsilon_h, \qquad (5)$$

that is, given three electronic levels ϵ_n, ϵ_p, and ϵ_h of the solid, ω is completely defined, independently of the frequency Ω of the photons which have been used to populate the given hole level ϵ_h. So, the easiest way to separate out from the total j the Auger contribution j_A, is to identify j_A with that part of the EDC which position in energy does not move when Ω is changed (while the proper photoemission EDC follows the variations of Ω). This is how we define formally the Auger current.

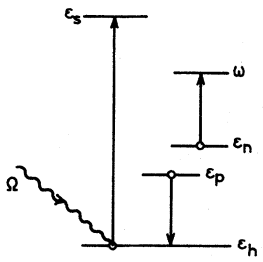

FIG. 1. Schematic energy representation of photon-induced Auger emission. A deep hole of energy ϵ_h is created by optical absorption of a photon Ω. The hole is filled by an electron from a higher state of energy ϵ_p, the excess energy thus released is used to excite the Auger electron from energy ϵ_n to ω.

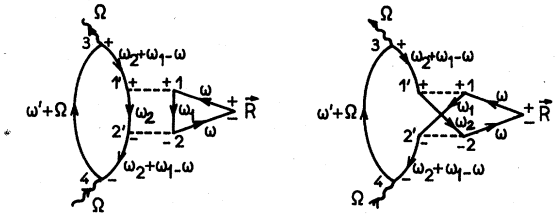

FIG. 2. Two lowest-order diagrams describing the photon-induced Auger current. Wavy lines stand for the electromagnetic field, full lines for electron propagators, and dotted ones represent Coulomb interactions. (a) Direct current j_d. (b) Exchange current j_{ex}.

The quantity $\mathcal{G}^{(2)+-}$ of Eq. (2) must be calculated up to second order in $\vec{A}$, and, in principle, to all orders in the Coulomb interaction V. This is easily formulated systematically with the help of Kjeldysh's perturbation theory for out-of-equilibrium many-body systems.[6] Using the corresponding diagrammatic expansion, it is easily checked that the contributions to j_A of lowest order in V are of order V^2. They correspond to the two diagrams of Fig. 2.

Figure 2(a) describes the direct Coulomb process, 2(b) the exchange one. Each solid line represents an element [determined by the values of the ($\pm$) indices] of the Kjeldysh one-electron matrix propagator[6] G of the noninteracting system in the absence of the electromagnetic field.

It is important to note that the choice of Kjeldysh ($\pm$) indices appearing in both diagrams is unique: the + and − indices at vertex $\vec{R}$ are imposed by expression (2) of the current. On the other hand, only electrons of energy ω larger than the vacuum energy—and henceforth larger than the Fermi energy μ of the solid—give a non-zero contribution to the current at infinity in the vacuum. This imposes, at zero temperature, that the electron-occupation propagator $\mathcal{G}_{\omega}^{+-}=0$, so that the indices at vertices $\vec{1}$ (and $\vec{1}'$) and $\vec{2}$ (and $\vec{2}'$) must be, respectively (+) and (−). This in turn entails ω_1 and $\omega_2<\mu$ (otherwise $\mathcal{G}_{\omega_1,\omega_2}^{+-}=0$), and $\omega'=\omega_1+\omega_2-\omega<\mu$. The same kind of argument fixes the remaining indices.

Finally, to lowest order in the Coulomb interaction, the angular and energy distribution of the Auger current reads (after summation on all internal spin indices)

$$j_A(\hat{R},\omega)=j_d(\hat{R},\omega)+j_{ex}(\hat{R},\omega)\,. \tag{6}$$

The direct term j_d is given by

$$\begin{aligned} j_d(\hat{R},\omega)=&\frac{1}{2\pi}\,\frac{4ie\hbar}{m}\left(\frac{e\hbar}{mc}\right)^2\left(\frac{\partial}{\partial R'}-\frac{\partial}{\partial R}\right)\\ &\times\int d\vec{1}\cdots d\vec{4}\,d\omega_1 d\omega_2 d\omega'\; G^r_{\omega}(\vec{R},\vec{1})\\ &\times G^a_{\omega}(\vec{2},\vec{R}')\,\mathrm{Im}G^r_{\omega_1}(\vec{1},\vec{2})V(\vec{1}-\vec{1}')V(\vec{2}-\vec{2}')\\ &\times \mathrm{Im}G^r_{\omega_2}(\vec{1}',\vec{2}')G^r_{\omega'}(\vec{2}',\vec{4})(\vec{a}\cdot\vec{\nabla})_4\mathrm{Im}G^r_{\omega'+\Omega}(\vec{4},\vec{3})(\vec{a}\cdot\vec{\nabla})_3 G^a_{\omega'}(\vec{3},\vec{1}')\Big|_{\substack{\vec{R}'\to\vec{R}\\ R\to\infty}}\\ &\times\delta(\omega+\omega'-\omega_1-\omega_2)\,\theta(\omega-E)\,\theta(\mu-\omega_1)\,\theta(\mu-\omega_2)\,, \end{aligned} \tag{7}$$

and the exchange term $j_{ex}(\vec{R},\omega)$ is obtained from expression (7) of j_d by multiplying it by a factor of $(-\frac{1}{2})$ and changing $\mathrm{Im}G^r_{\omega_1}(\vec{1},\vec{2})\mathrm{Im}G^r_{\omega_2}(\vec{1}',\vec{2}')$ into $\mathrm{Im}G^r_{\omega_1}(\vec{1},\vec{2}')\mathrm{Im}G^r_{\omega_2}(\vec{2},\vec{1}')$. G^r and G^a are the standard[6] retarded and advanced one-electron propagators of the noninteracting field-free system.

Before transforming (7) into a more explicit form, two remarks should be made:

(a) There are of course other contributions of order V^2 to the *total* current (2), but these do not belong to the Auger current. They do not describe a physical Auger process, except for the one depicted on Fig. 3. This diagram describes, in the presence of the Auger process of Fig. 1, the contribution to the current due to the "primary" electron excited up to state s by the photon, that it, in the usual terminology, a proper photoemission contribution.

(b) Obviously, it may be necessary to study corrections to j_A of order higher than V^2, e.g., if one wants to describe inelastic satellites of Auger lines. These are obtained formally by renormalizing the two diagrams of Fig. 2 in all possible ways. Note, however, that some of the terms thus obtained are ambiguous from the point of view of our definition of the Auger current: they are found among diagrams in which the "primary" line $\omega'+\Omega$ is connected by Coulomb interactions to the Auger electron lines ω. They correspond to terms in which, after the Auger process has taken place, the Auger electron in state $\phi_>$ (Fig. 1) and the primary one (state s) interact inelastically. However, these terms are very weak, due to the very small probability of such an interaction between two fast electrons with uncorrelated velocity directions.

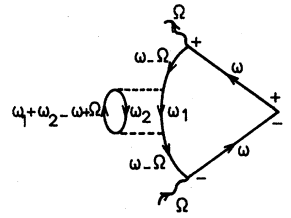

FIG. 3. Photoemission current in the presence of the Auger process of Fig. 1.

Let us now come back to rewriting Eq. (7) in terms of one-electron wave functions. Following Feibelman and Eastman,[5] we can write, for $\vec{R}$ at infinity in the vacuum.

$$G^r_{\omega}(\vec{R},\vec{1})=[G^a_{\omega}(\vec{1},\vec{R})]^*=-\frac{m}{2\pi\hbar^2}\,\frac{e^{ik_\omega R}}{R}\;\phi_>(\vec{1})\,, \tag{8}$$

where $k_\omega=[2m(\omega-E)/\hbar^2]^{1/2}$, and $\phi_>(\vec{1})$ is the wave function describing an electron of energy ω incoming from the vacuum onto the solid in direction $-\hat{R}$ (i.e., with wave vector $-k_\omega\hat{R}$), which is partly reflected back into the vacuum and partly transmitted into the solid.

Moreover, the other G^r and G^a appearing in Eq. (7) can be developed as

$$G^r_{\omega}(\vec{r},\vec{r}')=[G^a_{\omega}(\vec{r},\vec{r}')]^*=\sum_n\frac{\varphi_n^*(\vec{r})\varphi_n(\vec{r}')}{\omega-\epsilon_n+i\eta}\,, \tag{9}$$

with $\eta=0+$, and the φ_n's the wave functions of the one-electron eigen-states $|n\rangle$ of the semi-infinite solid plus vacuum system, of energies ϵ_n.

The direct and exchange parts of j_A can be written

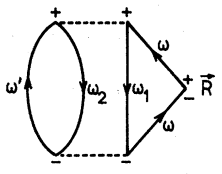

FIG. 4. Diagrammatic representation of $j_d^{(app)}$. The population of the deep-hole level (line ω') is the one created by optical absorption.

$$j_d(\hat{R},\omega)=K\sum_{\substack{n,p,s\\h,h'}}\frac{\langle np|V|h\phi_>\rangle\langle h|\vec{a}\cdot\vec{\nabla}|s\rangle\langle s|\vec{a}\cdot\vec{\nabla}|h'\rangle\langle\phi_>h'|V|pn\rangle}{(\epsilon_s-\Omega-\epsilon_h-i\eta)(\epsilon_s-\Omega-\epsilon_{h'}+i\eta)}$$
$$\times\delta(\epsilon_n+\epsilon_p-\omega-\epsilon_s+\Omega)\Theta(\omega-E)\Theta(\mu-\epsilon_n)\Theta(\mu-\epsilon_p)\,, \tag{10}$$

$$j_{ex}(\hat{R},\omega)=-\frac{K}{2}\sum_{\substack{n,p,s\\h,h'}}\frac{\langle np|V|h\phi_>\rangle\langle h|\vec{a}\cdot\vec{\nabla}|s\rangle\langle s|\vec{a}\cdot\vec{\nabla}|h'\rangle\langle\phi_>h'|V|np\rangle}{(\epsilon_s-\Omega-\epsilon_h-i\eta)(\epsilon_s-\Omega-\epsilon_{h'}+i\eta)}$$
$$\times\delta(\epsilon_n+\epsilon_p-\omega-\epsilon_s+\Omega)\Theta(\omega-E)\Theta(\mu-\epsilon_n)\Theta(\mu-\epsilon_p)\,, \tag{11}$$

where n, p, s, h, h' run on all possible electron states, the Coulomb matrix elements are defined by

$$\langle np|V|h\phi_>\rangle=\int d\vec{r}\,d\vec{r}'\,\varphi_n^*(\vec{r})\varphi_p^*(\vec{r}')\,V(\vec{r}-\vec{r}')\varphi_h(\vec{r}')\phi_>(\vec{r}) \tag{12}$$

and

$$K=\frac{em}{\hbar}\left(\frac{ie}{mc}\right)^2\frac{k_\omega}{R^2}\,. \tag{13}$$

We must now compare our expression of j_A with the one which is most ordinarily used to interpret experiments: the usual theory[1] whould correspond to the diagram of Fig. 4, in which the population of the deep-hole level (line ω') would be the one created by optical absorption. Namely, it is written as the product of the optical-transition probability per unit time and the lifetime of the deep hole. This, in our present lowest-order calculation, is simply[1] $\eta^{-1}\to\infty$ (lifetime effects will be discussed in Sec. IV). This gives, for the direct current,

$$j_d^{(app)}(\hat{R},\omega)=\frac{\pi K}{\eta}\sum_{n,p,s,h}|\langle np|V|h\phi_>\rangle\langle h|\vec{a}\cdot\vec{\nabla}|s\rangle|^2\delta(\epsilon_h+\Omega-\epsilon_s)$$
$$\times\delta(\epsilon_n+\epsilon_p-\epsilon_h-\omega)\Theta(\omega-E)\Theta(\mu-\epsilon_n)\Theta(\mu-\epsilon_p)\,. \tag{14}$$

It is seen that the main difference between expressions (14) and (10) is the following: for given n, p, s, the exact expression (10) involves the square of the sum on deep-hole h states of the probability *amplitude* $\langle np|V|h\phi_>\rangle\langle h|\vec{a}\cdot\vec{\nabla}|s\rangle$ of the full process shown in Fig. 1, while $j_d^{(app)}$ only contains an incoherent sum of probability *intensities*. Formally, this derives from the fact that the exact diagram (2a) contains two deep-hole ω' lines, while the approximate one (Fig. 4) only has one. As was pointed out in Sec. I, the exact expression takes into account the fact that the deep holes are excited coherently by the photon field, and that the intermediate electron (state p) fills the state made of a coherent superposition of holes thus created. So, the Auger current is itself built up by addition of coherent electron waves emitted in state $\phi_>$ from the various h hole states. This gives rise to the interference contributions $h\neq h'$ to the exact current (10), which are neglected in $j^{(app)}$.

From now on, we will only consider, for simplicity, the Auger processes involving narrow (i.e., deep) hole levels. First of all, it is easily seen by studying the energy denominator of expression (10) that the ratio of the contribution of interference terms between hole states with $\epsilon_{h'}\neq\epsilon_h$ to that of states $\epsilon_{h'}=\epsilon_h$ is of order $\eta/(\epsilon_{h'}-\epsilon_h)\to 0$. Therefore, only interferences between degenerate deep-hole states have to be considered here. The exact Auger current then appears as the sum of the contributions of the various deep-hole energy levels. The direct current due to processes involving the hole level ϵ_h reads

$$j_d(\hat{R},\omega,\epsilon_h)=\frac{\pi K}{\eta}\sum_{n,p,s}\Big|\sum_h{}'\,\langle np|V|h\phi_>\rangle\langle h|\vec{a}\cdot\vec{\nabla}|s\rangle\Big|^2\delta(\epsilon_s-\Omega-\epsilon_h)$$
$$\times\delta(\epsilon_n+\epsilon_p-\omega-\epsilon_h)\Theta(\omega-E)\Theta(\mu-\epsilon_n)\Theta(\mu-\epsilon_p)\,, \tag{15}$$

where the restricted sum $\sum_h'$ only runs on the degenerate states of energy ϵ_h. It is seen in Eq. (15) that the diagonal ($h'\equiv h$) terms reproduce identically the usual approximate expression (14), which will therefore be correct only when interference terms can be proved to be negligible.

Finally, the same conclusions hold for the exchange current,

$$j_{ex}(R,\omega,\epsilon_h)=-\frac{\pi K}{2\eta}\sum_{n,p,s}\sum_{h,h'}{}'\,\langle np|V|h\phi_>\rangle\langle h|\vec{a}\cdot\vec{\nabla}|s\rangle\langle s|\vec{a}\cdot\vec{\nabla}|h'\rangle\langle\phi_>h'|V|np\rangle\delta(\epsilon_s-\Omega-\epsilon_h)$$
$$\times\delta(\epsilon_n+\epsilon_p-\omega-\epsilon_h)\Theta(\omega-E)\Theta(\mu-\epsilon_n)\Theta(\mu-\epsilon_p)\,. \tag{16}$$

Before considering interference effects in more detail, let us make one final remark about corrections to j_A of order higher than V^2: coming back to the exact diagrams of Fig. 2, it is seen that there exist renormalization terms in which the two deep-hole ω' lines are connected by interaction lines. These terms cannot appear in the renormalization of the approximate diagram (Fig. 4), where one can only renormalize *separately* the optical-and the Auger-transition probabilities. So, even if expression (10) happens to be exact to order V^2 (i.e., in cases with zero interferences), it may not remain correct to higher orders in V. Note that the terms which couple the two deep lines (at the same energy ω') are in general non-negligible with respect to the separate renormalizations of the two lines.[2,3]

III. INTERFERENCES IN THE INFINITE-LIFETIME LIMIT

In this section we classify and study qualitatively in some simple examples the interference terms which appear in the Auger current, to lowest order in the Coulomb interaction. Since we have assumed the deep holes to be localized in space, the restricted sums $\sum_h'$ in Eqs. (15) and (16) only involve hole states with the same energy ϵ_h. The corresponding degeneracy can be of two types:

(i) $|h\rangle$ and $|h'\rangle$ correspond to two atomic orbitals localized on two different atomic sites. The corresponding term will be called "extra-atomic interference."

(ii) $|h\rangle$ and $|h'\rangle$ are two different atomic orbitals on the same atomic site. The corresponding term we call "intra-atomic interference." This degeneracy corresponds, for example, in simple cases, to various orbital angular momentum orientations. (Note that when spin-orbit coupling is negligible, the spin degeneracy does not induce interferences, due to the fact that the Coulomb interaction is spin independent.)

In order to illustrate the effect of the two kinds of degeneracy, we will now consider in more detail two particularly simple examples:

A. Narrow Auger line

This is the case where the three levels n, p, h are infinitely narrow, i.e., where states n, p, h are completely localized atomic states. The associated wave functions, e.g., $\varphi_p(\vec{r}-\vec{R}_\lambda)$, will be denoted by $|p_\lambda\rangle$. (That is, from now on, n, p, h will label the various atomic orbitals, and subscripts λ, μ... the atomic sites.) We will call $(\epsilon_h, \epsilon_n, \epsilon_p)$ the corresponding line. In this case, the physical information is contained in the angular distribution of j_A at the line energy $\omega = \epsilon_n + \epsilon_p - \epsilon_h$.

Since we neglect the overlap of φ_n, φ_p, φ_h on different sites, the Coulomb matrix element $\langle n_\mu p_\nu | V | h_\lambda \phi_> \rangle$ is nonzero only when states φ_p and φ_h are centered on the same site, i.e., when

$$\langle n_\mu p_\nu | V | h_\lambda \phi_> \rangle = \delta_{\lambda\nu} \int d\vec{r}\, d\vec{r}'\, \varphi_n^*(\vec{r}-\vec{R}_\mu) \times \varphi_p^*(\vec{r}'-\vec{R}_\lambda) V(\vec{r}-\vec{r}') \times \varphi_h(\vec{r}'-\vec{R}_\lambda)\phi_>(\vec{r}) . \quad (17)$$

The relevant Coulomb interaction is the Coulomb potential screened by the dielectric constant at the frequency $(\epsilon_p - \epsilon_h)$ of the Auger transition. In general this is much larger than the plasma frequency, so that the screening is quite poor, and the range of V is much larger than the atomic distance. Therefore, in Eq. (17), $\vec{r}$ may run on several atomic cells around $\vec{R}_\lambda$. The effect of contributions $\lambda \neq \mu$ to the Coulomb matrix element (17) has been studied in detail by Citrin *et al.*[7] We will call them *intersite* contributions. Note that, if both $|h\rangle$ and $|p\rangle$ have zero angular momentum, these intersite contributions are zero (or, more exactly, exponentially small) as a result of Gauss's theorem (since the spherically symmetric electronic distribution $\varphi_p^* \varphi_h$ corresponds to a zero total electric charge).

(a) *Direct current.* From Eqs. (15) and (17), we get

$$j_d(\hat{R}, \omega, (\epsilon_h, \epsilon_n, \epsilon_p)) = \frac{\pi K}{\eta} \sum_{\substack{n,p,s \\ h,h',\lambda,\mu}}{}' \delta(\epsilon_n + \epsilon_p - \omega - \epsilon_h)(\langle n_\mu p_\lambda | V | h_\lambda \phi_> \rangle \langle \phi_> h'_\lambda | V | p_\lambda n_\mu \rangle + \langle p_\mu n_\lambda | V | h_\lambda \phi_> \rangle \langle \phi_> h'_\lambda | V | n_\lambda p_\mu \rangle) \times \langle h_\lambda | \vec{a}\cdot\vec{\nabla} | s \rangle \langle s | \vec{a}\cdot\vec{\nabla} | h'_\lambda \rangle , \quad (18)$$

where the sum $\sum'$ is restricted to states with fixed ϵ_n, ϵ_p, ϵ_h, and $\epsilon_s = \epsilon_h + \Omega$.

Therefore, j_d contains no extra-atomic interferences: this results from the localization of the (common) intermediate state p_λ or n_λ, which cannot interact in the same process with two holes on different sites. So, the only possible interferences are those associated with an atomic degeneracy of the hole level. We will illustrate them on the example of orbital degeneracy, which implies $L_h \neq 0$. Let us specialize to the simplest case: $L_h = 1$, $L_n = L_p = 0$. $|\phi_>\rangle$ and $|s\rangle$ will be approxi-

mated by plane waves with respective wave vectors $\vec{q}$ and $\vec{s}$.

(i) *Intrasite contribution* ($\vec{R}_\mu = \vec{R}_\lambda$). The h states correspond to the three values $m = 0, \pm 1$, of $L_h^{(z)}$. The matrix elements have the form

$$\langle n_\lambda p_\lambda \mid V \mid m_\lambda \phi_\lambda \rangle = C Y_{1m}^*(\hat{q}) e^{i\vec{q}\cdot\vec{R}_\lambda}, \tag{19}$$

$$\langle m_\lambda \mid \vec{a}\cdot\vec{\nabla} \mid \vec{s}\rangle = C' Y_{1m}(\hat{s})(\hat{s}\cdot\vec{a}) e^{i\vec{s}\cdot\vec{R}_\lambda}, \tag{20}$$

where $\hat{q}$ and $\hat{s}$ are the unit vectors along directions $\vec{q}$ and $\vec{s}$. The constants C and C' depend only on the energies of the five relevant levels (Fig. 1), but not on the direction of $\hat{s}$, which is to be integrated on. The $\hat{q}$ direction is the refracted associate of the direction of observation $\hat{k} = -k_\omega \hat{R}$.

Finally, the intrasite term in j_d has the form

$$j_d^{(\mathrm{intra})}(\hat{R}, \omega, (\epsilon_h, \epsilon_n, \epsilon_p)) \propto a^2 + 2(\vec{a}\cdot\hat{q})^2, \tag{21}$$

that is, it exhibits a conical symmetry around the direction of $\vec{a}$ inside the solid, the distribution in the vacuum being the refracted associate of (21).

For comparison, one can calculate the intrasite term which would result if interferences ($m' \neq m$) were neglected. It has the angular distribution

$$a^2 + 2(a_x^2 \hat{q}_x^2 + a_y^2 \hat{q}_y^2 + a_z^2 \hat{q}_z^2), \tag{22}$$

i.e., it is not invariant under a rotation of the coordinate frame. This is obviously unphysical since, in the present model, the Auger processes occur independently on atoms without any preferred direction but $\vec{a}$.

It is interesting, at this stage, to compare the above results with the direct intrasite current obtained in the case $L_h = L_n = 0$, $L_p = 1$, where the charge fluctuation (hp) has the same angular momentum ($L = 1$), but which is interference-free since the hole state is nondegenerate. This is easily found to be spherical ($\propto a^2$).

So, it appears that the angular distribution is strongly affected by intra-atomic interferences, which modify its amplitude and even its symmetry.

(ii) *Intersite contribution* ($\vec{R}_\mu \neq \vec{R}_\lambda$). Case $L_h = 1$, $L_n = L_p = 0$. Since the charge fluctuation $\varphi_p^* \varphi_h$ has a dipolar character (with associated dipole strength π_λ), the Coulomb matrix elements is the interaction energy between this dipole and the charge distribution $\varphi_n^* \phi_\lambda$ localized around site μ. So, its main term is the dipole-dipole interaction energy between $\vec{\pi}_\lambda$ and the dipole $\vec{\pi}'_\mu$ of $\varphi_n^* \phi_\lambda$. We then obtain

$$\sum_m \langle n_\mu p_\lambda \mid V \mid m_\lambda \phi_\lambda \rangle \langle m_\lambda \mid \vec{a}\cdot\vec{\nabla} \mid s\rangle = C_{\mu\lambda} \frac{\pi_\lambda \pi'_\mu}{R_{\mu\lambda}^3} e^{i(\vec{s}\cdot\vec{R}_\lambda + \vec{q}\cdot\vec{R}_\mu)} \times (\hat{s}\cdot\hat{a})[\hat{s}\cdot\hat{q} - 3(\hat{q}\cdot\hat{R}_{\lambda\mu})(\hat{s}\cdot\hat{R}_{\lambda\mu})], \tag{23}$$

with $\vec{R}_{\lambda\mu} = \vec{R}_\lambda - \vec{R}_\mu$.

After integration on the direction $\hat{s}$ of the primary electron, we thus get, for the contribution of the first nearest neighbors in a cubic lattice of lattice distance b, with cubic axes along $\hat{x}, \hat{y}, \hat{z}$, the angular distribution

$$j_d^{(\mathrm{inter})}(\hat{R}, \omega, (\epsilon_h, \epsilon_n, \epsilon_p)) \propto b^{-6}[a^2 + 3(a_x^2 \hat{q}_x^2 + a_y^2 \hat{q}_y^2 + a_z^2 \hat{q}_z^2) - (\vec{a}\cdot\hat{q})^2]. \tag{24}$$

This expression is not invariant under a rotation of the reference frame, since we are dealing with two-site processes and have chosen the reference frame to be tied to the physical lattice. Of course, as expected, $j_d^{(\mathrm{inter})}$ has the (cubic) symmetry of the lattice. Note again, for comparison, that in the reverse case ($L_h = L_n = 0$, $L_p = 1$), the analogous nearest-neighbor term can be shown to have a spherical distribution.

(b) *Exchange current.* It is given by Eq. (16). The relevant Coulomb matrix elements are

$$\langle n_\mu p_\nu \mid V \mid h_\lambda \phi_\lambda \rangle \langle \phi_{\lambda'} h'_{\lambda'} \mid V \mid n_\mu p_\nu \rangle,$$

so that the overlap restriction (17) imposes $\nu = \lambda$, $\mu = \lambda'$, and two cases are possible.

(1) No (or negligible) intersite interaction: $\lambda = \mu = \lambda'$, and there are only intra-atomic interferences. For example, if $L_h = 1$, $L_n = L_p = 0$, one finds for j_{ex} the same angular distribution as for $j_d^{(\mathrm{intra})}$ [Eq. (21)]. Again, if interferences would be neglected, one would find the unphysical result (22).

(2) There is a non-negligible intersite matrix element: the terms $\lambda \neq \lambda'$ are now nonzero, and correspond to extra-atomic interferences induced by the intersite interaction. The corresponding distribution, for $L_h = 1$, $L_n = L_p = 0$ is a complicated function of $\vec{a}$, $\hat{q}$, and $\vec{R}_{\lambda\lambda'}$. For $sR_{\lambda\lambda'} \gg 1$ (where $\hbar^2 s^2/2m = \epsilon_h + \Omega$), the contribution of the pair of sites (λ, λ') reduces to

$$R_{\lambda\lambda'}^{-6} e^{i\vec{q}\cdot\vec{R}_{\lambda\lambda'}} \frac{\sin(sR_{\lambda\lambda'})}{sR_{\lambda\lambda'}} (\vec{a}\cdot\hat{R}_{\lambda\lambda'})^2 (\hat{q}\cdot\hat{R}_{\lambda\lambda'})^2 \tag{25}$$

B. n and p belong to a wide band: (atomic V-V line)

For simplicity, since we are mainly interested here in the effect of delocalization of the intermediate states, we will assume that the atomic orbital $|h\rangle$ is nondegenerate and we are left with only the site degeneracy of the hole state (this describes for example the case of a KVV line).

We now denote states $|n\rangle$ and $|p\rangle$ by their reduced wave vectors $\vec{k}$ and $\vec{K}$ and, as is most usually done, approximate them by the Bloch wave functions of the infinite solid: $\varphi_{\vec{k}}(\vec{r}) = u_{\vec{k}}(\vec{r}) e^{(i\vec{k}\cdot\vec{r})}$. The Coulomb matrix elements appearing in the direct current are

$$\langle np \,|\, V \,|\, h_\lambda \phi_> \rangle \langle \phi_> h_{\lambda'} \,|\, V \,|\, pm \rangle \equiv \langle \vec{K}\vec{k} \,|\, V \,|\, h_\lambda \phi_> \rangle \langle \phi_> h_{\lambda'} \,|\, V \,|\, \vec{k}\vec{K} \rangle . \quad (26)$$

Since $|\vec{k}\rangle$ is an extended state, it has overlaps of the same amplitude with the localized states $|h_\lambda\rangle$ and $|h_{\lambda'}\rangle$, thus giving rise to extra-atomic interferences. Making use of the periodicity of $u_{\vec{k}}(\vec{r})$, one finds

$$j_d(\hat{R}, \omega, (\epsilon_h VV)) = \frac{\pi K}{\eta} \sum_{\substack{\vec{k}\vec{K}\vec{s} \\ \lambda\lambda'}} |M(\vec{q}, \vec{k}, \vec{K}) C(\vec{s})|^2 \, e^{i(\vec{q}+\vec{s}-\vec{k}-\vec{K})\cdot\vec{R}_{\lambda\lambda'}} \times \delta(\epsilon_s - \Omega - \epsilon_h)\delta(\epsilon_{\vec{k}}^* + \epsilon_{\vec{K}} - \omega - \epsilon_h) , \quad (27)$$

where

$$C(\vec{s}) = \int d\vec{\rho} e^{-i\vec{s}\cdot\vec{\rho}} \vec{a}\cdot\vec{\nabla}\varphi_h(\vec{\rho}) , \quad (28)$$

$$M(\vec{q}, \vec{k}, \vec{K}) = \int d\vec{\rho}\, d\vec{\rho}' e^{i(\vec{q}-\vec{K})\cdot\vec{\rho}'} u_{\vec{k}}^*(\vec{\rho}') \times V(\vec{\rho} - \vec{\rho}') e^{-i\vec{k}\cdot\vec{\rho}} u_{\vec{k}}^*(\vec{\rho})\varphi_h(\vec{\rho}) . \quad (29)$$

Note that M can be separated into intra- and intersite parts: $\vec{\rho}$ in Eq. (29) is limited to one atomic cell, while the range $\vec{\rho}'$ is only limited by the range of V.

Assuming M and C to be quasiconstant, we see that, if we neglect interferences (i.e., only keep terms $R_{\lambda\lambda'} = 0$) j_d reduces to

$$j_d^{(\mathrm{app})}(\hat{R}, \omega, (\epsilon_h VV)) = \frac{\pi K}{\eta} |MC|^2 N\rho_s(\epsilon_h + \Omega) \times \int d\omega_1 \rho_V\left(\omega_1 + \frac{\omega + \epsilon_h}{2}\right) \times \rho_V\left(\frac{\omega + \epsilon_h}{2} - \omega_1\right), \quad (30)$$

where N is the number of atoms in the solid, and ρ_s and ρ_V are, respectively, the density of primary and valence states. As expected, we find the well-known result of the approximate theory,[8] i.e., a line shape proportional to the autoconvolution of ρ_V. Moreover, within the approximation $|M| = cst$, the corresponding angular distribution is spherical inside the solid (i.e., conical around the normal to the surface in the vacuum).

On the other hand, the exact expression can be rewritten

$$j_d(\hat{R}, \omega, (\epsilon_h VV)) = \frac{\pi K}{\eta} |MC|^2 \sum_{\lambda\lambda'} e^{i\vec{q}\cdot\vec{R}_{\lambda\lambda'}} \bar{A}_s(\epsilon_h + \Omega, \vec{R}_{\lambda\lambda'}) \int d\omega_1 \bar{A}_V\left(\frac{\omega + \epsilon_h}{2} + \omega_1, \vec{R}_{\lambda\lambda'}\right) \bar{A}_V\left(\frac{\omega + \epsilon_h}{2} - \omega_1, \vec{R}_{\lambda\lambda'}\right) , \quad (31)$$

where

$$\bar{A}_V(\omega, \vec{R}_{\lambda\lambda'}) = \sum_{\vec{k}} \delta(\omega - \epsilon_{\vec{k}}) e^{-i\vec{k}\cdot\vec{R}_{\lambda\lambda'}} \quad (32)$$

and a similar expression for $\bar{A}_s$.

The quantities $\bar{A}_s(\vec{R}_{\lambda\lambda'})$ and $\bar{A}_V(\vec{R}_{\lambda\lambda'})$ can be interpreted qualitatively as "cell-averaged spectral densities" of the primary and valence states. Indeed, calling $\bar{A}(\vec{r}, \vec{r}', \omega)$ the exact spectral densities, we find

$$\int d\vec{r}\, d\vec{r}' \, A(\vec{r}, \vec{r}', \omega) = \sum_{\vec{k}\lambda\lambda'} \delta(\omega - \epsilon_{\vec{k}}) e^{i\vec{k}\cdot\vec{R}_{\lambda\lambda'}} |\beta(\vec{k})|^2 \equiv \sum_{\lambda\lambda'} \langle A \rangle_{\lambda\lambda'} \quad (33)$$

with

$$\beta(\vec{k}) = \int_{\text{one cell}} d\vec{r}\, \varphi_{\vec{k}}(\vec{r}) ,$$

and, in our approximation of quasiconstant matrix elements $\bar{A}(\vec{R}_{\lambda\lambda'})$ is simply proportional to $\langle A \rangle_{\lambda\lambda'}$.

So, j_d is the sum of contributions of all site pairs (λ, λ'), each interference term $(\lambda' \neq \lambda)$ being proportional to the autoconvolution of the cell-averaged spectral density $\bar{A}_V(\omega, \vec{R}_{\lambda\lambda'})$. However, the term related to the optical transition, $\bar{A}_s(\epsilon_h + \Omega, \vec{R}_{\lambda\lambda'})$ does not factor out of the $\vec{R}_{\lambda\lambda'}$ sum, so that the line shape depends on the photon frequency. Moreover, the angular distribution explicitly depends on $\vec{q}$, and its symmetries are, inside the solid, those of the crystal lattice.

One may wonder whether, as is sometimes stated,[9] the approximate expression (30) becomes exact when the primary energy $\epsilon_s = \epsilon_h + \Omega$ is very large compared with the valence-band energies and with ω. In order to make that point clear, let us consider the $\vec{R}_{\lambda\lambda'}$ dependence of the $\bar{A}$'s. Assuming primary states to be plane waves, one has

$$\bar{A}_s(\epsilon_s, \vec{R}_{\lambda\lambda'}) = \rho_s(\epsilon_s) \frac{\sin(sR_{\lambda\lambda'})}{sR_{\lambda\lambda'}} , \quad (34)$$

with $\hbar^2 s^2/2m = \epsilon_s$. Anisotropic band effects make $\bar{A}_V(\omega, \vec{R}_{\lambda\lambda'})$ more complicated, but it always behaves roughly, at large distances $(R_{\lambda\lambda'} \gg [k_0(\omega)]^{-1}$, where $k_0(\omega)$ is a characteristic radius of the constant-energy surface S_ω), as $(k_0 R_{\lambda\lambda'})^{-1}$ osc$(k_0 R_{\lambda\lambda'})$.[10] So, the lattice sum of Eq. (31) does converge. If s is much larger than q and all the k_0's appearing

in the $\bar{A}_V$'s, $\bar{A}_s$ oscillates with $R_{\lambda\lambda'}$ much faster than the valence band factor and than $\exp(i\vec{q}\cdot\vec{R}_{\lambda\lambda'})$. If the $R_{\lambda\lambda'}$'s would be continuously distributed in space, this would entail that the only nonzero contribution to j_d would be the $R_{\lambda\lambda'}=0$ one, and $j^{(\mathrm{app})}$ would become exact. However, the $R_{\lambda\lambda}$'s corresponding to near neighbors have a finite spacing of the order of the lattice distance $b \gg s^{-1}$, so that the contributions of near-neighbor interferences do not average out (this only occurs for terms with $R_{\lambda\lambda'}/b \gg sb$), and interference effects in j_d do not wash out. The same analysis can be made on the exchange current, obviously yielding the same qualitative results.

IV. LIFETIME EFFECTS

The question now arises of estimating the importance of interferences in real solids, where interactions give rise to finite lifetimes and mean-free paths for all the states involved in the Auger emission process. Finite lifetimes result in uncertainties on phases, which certainly affect the phase coherence responsible for interference effects.

Of course, as was mentioned in Sec. II, interactions also give rise to a variety of other effects (inelastic Auger current, scattering between Auger and primary electrons, indirect transitions, correlations of higher orders...) which must, in principle, also be taken into account in order for conservation laws to be satisfied. However, in the present article, we will neglect them and only take into account interactions by introducing phenomenologically finite lifetimes for all the states involved in the process—i.e., we keep to separate renormalizations of the various lines of the bare Auger diagrams (Fig 2).

For the sake of clarity, we first examine separately the effect of the finite lifetime of each level.

A. Lifetime of the Auger electron

The wave function $\phi_>$ describing the Auger electron is still built by starting from an incident plane wave of wave vector $-k_\omega \hat{R}$ on the vacuum side. Since $\phi_>$ must be continuous along the surface plane, the parallel component $\vec{q}_{\parallel}$ of its wave vector $\vec{q}$ inside the solid is still real: Its transverse component is given by

$$(\hbar^2/2m)q_\perp^2 = \omega + i\Gamma_\omega - (\hbar^2/2m)q_\parallel^2 , \tag{35}$$

where $\tau_\omega = \hbar\Gamma_\omega^{-1}$ is the lifetime of an electron at energy ω. So, $q_\perp$ has an imaginary part $q_\perp^{(i)}$, which corresponds to an attenuation of the wave $\phi_>$ in the transverse direction:

$$q_\perp^{(i)} \simeq (2m/\hbar^2)^{1/2}(\Gamma_\omega/2\omega^{1/2}\cos\theta) , \tag{36}$$

where θ is the angle between $\vec{q}$ and the normal to the surface. That is, $\phi_>$ has a constant extinction coefficient $(2m/\hbar^2)^{1/2}(\Gamma_\omega/2\omega^{1/2})$ along its direction of propagation.

When included in the calculation of the Coulomb matrix element, this extinction effect results, for the contribution of a pair of sites (λ,λ') to the Auger current, in a factor $\exp[-q_\perp^{(i)}(R_{\lambda\perp}+R_{\lambda'\perp})]$, where $R_{\lambda\perp}$ is the distance from site λ to the surface.

This means that the effective region of emission of the (elastic) Auger current is a layer along the surface of thickness $l_\omega\cos\theta$,[11] where the mean free path $l_\omega = (\hbar^2/2m)^{1/2}(2\omega^{1/2}/\Gamma_\omega)$. So, for terms corresponding to extra-atomic interferences, both sites λ and λ' are limited to this extraction depth but the extinction effect does not limit the distance $\vec{R}_{\lambda\lambda',\parallel}$ between them in the direction parallel to the surface. That is, the two waves emitted from $\vec{R}_\lambda$ and $\vec{R}_{\lambda'}$ are separately attenuated along their "optical path," but a finite Γ_ω does not affect their relative phases.

B. Deep-hole lifetime

Introducing a finite deep-hole linewidth Γ simply amounts to changing, in Eqs. (10) and (11), η into Γ. Assuming that Γ is the same for all deep-hole states, one gets for the direct current:

$$\begin{aligned} j_d(\hat{\vec{R}},\omega,\epsilon_h) = \frac{\pi K}{\Gamma}\sum_{\substack{nps\\ hh'}} & \langle np\,|\,V\,|h\phi_>\rangle\langle h\,|\,\vec{a}\cdot\vec{\nabla}\,|s\rangle\langle s\,|\,\vec{a}\cdot\vec{\nabla}\,|h'\rangle \\ & \times\langle\phi_> h'\,|\,V\,|pn\rangle\,\frac{\Gamma/\pi}{(\epsilon_s-\Omega-\epsilon_h+i\Gamma)(\epsilon_s-\Omega-\epsilon_{h'}-i\Gamma)} \\ & \times\delta(\epsilon_n+\epsilon_p-\omega-\epsilon_s+\Omega)\theta(\omega-E)\theta(\mu-\epsilon_n)\theta(\mu-\epsilon_p) \end{aligned} \tag{37}$$

and a similar expression for j_{ex}.

Equation (37) shows that the presence of a finite Γ has three main physical consequences:

(i) As expected, it makes the Auger current finite (the effective hole population is that due to optical transitions during the lifetime $\tau=\hbar/\Gamma$).

(ii) Consider two nondegenerate hole states of energies ϵ_h, $\epsilon_{h'}$. The ratio of the contribution of interferences between these two states to that of states $\epsilon_{h'} = \epsilon_h$ is of order $\Gamma/(\epsilon_{h'} - \epsilon_h)$. So, now interferences are no longer limited to strictly degenerate hole states, but only to quasidegenerate states with an energy separation smaller than the sum of their widths.

(iii) The last, and most interesting effect, is the limitation of the space range of extra-atomic interferences. In order to illustrate this effect, let us come back to the second example of Sec. III, where states $|n\rangle$ and $|p\rangle$ both belong to the same wide band. Expression (31) becomes

$$j_d(\hat{\vec{R}}, \omega, (\epsilon_h VV)) = \frac{\pi K}{\Gamma} |MC|^2 \sum_{\lambda\lambda'} e^{i\vec{q}\cdot\vec{R}_{\lambda\lambda'}} \sum_{\vec{s}} \frac{(\Gamma/\pi) e^{i\vec{s}\cdot\vec{R}_{\lambda\lambda'}}}{(\epsilon_s - \Omega - \epsilon_h)^2 + \Gamma^2} \times \int d\omega_1 \bar{A}_V\left(\frac{\omega + \epsilon_s - \Omega}{2} + \omega_1, \vec{R}_{\lambda\lambda'}\right) \bar{A}_V\left(\frac{\omega + \epsilon_s - \Omega}{2} - \omega_1, \vec{R}_{\lambda\lambda'}\right). \tag{38}$$

Integration on $\vec{s}$ (with $\epsilon_s = \hbar^2 s^2/2m$) immediately gives

$$j_d(\hat{\vec{R}}, \omega, (\epsilon_h VV)) = \frac{\pi K}{\Gamma} |MC|^2 \sum_{\lambda\lambda'} e^{i\vec{q}\cdot\vec{R}_{\lambda\lambda'}} \bar{\mathfrak{A}}_s(\epsilon_h + \Omega, \vec{R}_{\lambda\lambda'}) \times \int d\omega_1 \bar{\mathfrak{A}}_V\left(\frac{\omega + \epsilon_h}{2} + \omega_1, \vec{R}_{\lambda\lambda'}\right) \bar{\mathfrak{A}}_V\left(\frac{\omega + \epsilon_h}{2} - \omega_1, \vec{R}_{\lambda\lambda'}\right). \tag{39}$$

The average spectral densities $\bar{\mathfrak{A}}$ are now defined by

$$\bar{\mathfrak{A}}_V(\omega, \vec{R}_{\lambda\lambda'}) = \sum_{\vec{k}} \frac{\Gamma/\pi}{(\omega - \epsilon_{\vec{k}})^2 + \Gamma^2} e^{i\vec{k}\cdot\vec{R}_{\lambda\lambda'}} \tag{40}$$

$$\bar{\mathfrak{A}}_s(\epsilon_h + \Omega, \vec{R}_{\lambda\lambda'}) = \rho_s(\epsilon_h + \Omega) \times \frac{\sin(s_0 R_{\lambda\lambda'})}{s_0 R_{\lambda\lambda'}} e^{-s_1 R_{\lambda\lambda'}} \tag{41}$$

with $\rho_s(\epsilon_h + \Omega) = m s_0/2\pi^2\hbar^2$, and s_0 and s_1 are given, for $\Gamma \ll \epsilon_h + \Omega$, by

$$s_0 = \left(\frac{2m(\epsilon_h + \Omega)}{\hbar^2}\right)^{1/2},$$

$$s_1 = \Gamma\left(\frac{m}{2\hbar^2(\epsilon_h + \Omega)}\right)^{1/2} \equiv \frac{\hbar\Gamma}{v_g(\epsilon_s)}. \tag{42}$$

It is seen that $\bar{\mathfrak{A}}_s$ decreases exponentially with increasing $R_{\lambda\lambda'}$, with a characteristic range s_1^{-1}. It is easy to show that, whatever the details of the valence-band shape, $\bar{\mathfrak{A}}_V(\omega, \vec{R}_{\lambda\lambda'})$ has a similar behavior at large distances, with a characteristic range of order $\hbar\bar{v}_g(\omega)/\Gamma$, where $\bar{v}_g(\omega)$ is some average group velocity of an electron of energy ω.

Therefore, each of the three "spectral densities" $\bar{\mathfrak{A}}$ of expression (39) introduces a cutoff for the space range of extra-atomic interferences, so that their effective range is determined by the smallest of these three distances.

This cutoff effect can be easily interpreted: the various deep-hole "sources" have a finite coherence time $\tau = \hbar/\Gamma$. In order for interferences to be possible, it is necessary that the times of propagation of states $|\vec{s}\rangle$, $|\vec{k}\rangle$, $|\vec{K}\rangle$ between $\vec{R}_\lambda$ and $\vec{R}_{\lambda'}$ be smaller than τ, i.e.,

$$t_{\lambda\lambda'} = R_{\lambda\lambda'}/v_g < \hbar/\Gamma \quad \text{or} \quad R_{\lambda\lambda'} < \hbar v_g/\Gamma.$$

This interpretation shows that the relative amplitude of intra-atomic interference terms with respect to noninterference ones is not affected by the deep-hole lifetime [which can easily be checked, e.g., by Eq. (18)]. Indeed, the phase coherence between two holes states localized on the same site remains perfect. It is only the *total* intra-atomic intensity, line shape, and angular distribution which are modified.

C. Lifetimes of primary and intermediate states

Introducing a finite lifetime $\Gamma_{s,n,p}$ for one of these states simply amounts to writing for the corresponding $\mathrm{Im}G^r$ of Eq. (7) the exact broadened spectral density. This results, for the case of an atomic-V–V-line, in the replacement in Eq. (31) of the corresponding $\bar{A}$ by the proper broadened quantity:

$$\bar{\mathfrak{A}}_s(\omega, \vec{R}_{\lambda\lambda'}) = \sum_{\vec{s}} \frac{\Gamma_s/\pi}{(\omega - \epsilon_{\vec{s}})^2 + \Gamma_s^2} e^{i\vec{s}\cdot\vec{R}_{\lambda\lambda'}},$$

$$\bar{\mathfrak{A}}_V(\omega, \vec{R}_{\lambda\lambda'}) = \sum_{\vec{k}} \frac{\Gamma_k/\pi}{(\omega - \epsilon_{\vec{k}})^2 + \Gamma_k^2} e^{i\vec{k}\cdot\vec{R}_{\lambda\lambda'}}. \tag{43}$$

So, as was discussed above, each of these Γ's introduces a cutoff for the space range of extra-atomic interferences:

$$l_i = \hbar v_g^{(i)}/\Gamma_i \quad (i = \vec{s}, \vec{k}, \vec{K}). \tag{44}$$

These cutoffs are therefore determined by the phase blurring of each of the three states itself.

Obviously, in practice, all the above effects combine to fix the effective interference range. So, it can be concluded that (i) The extraction depth of the Auger current is determined by the mean

free path l_ω of the outgoing Auger electron. (ii) The relative strength of intra-atomic interferences is not affected by lifetime effects so that, if the atomic deep-hole state is (quasi-) degenerate, they should always be taken into account. (iii) The range of extra-atomic interferences is limited to the smallest of the lengths l_i and l_i' $(i=s,n,p)$, where the l_i's are the mean free paths of the primary and intermediate states, while the l_i''s $(l_i'=\hbar v_g^{(i)}/\Gamma)$ are the distances on which they propagate during the lifetime τ of the deep hole.

In general, the smallest of these lengths are l_n' and l_p' (except if the primary electrons are in the far-uv range where l_s becomes smaller than the atomic distance). Taking as an order of magnitude $\epsilon_{\vec{k}}^* - E_0 \sim 7$ eV, $b=3$Å (where E_0 is the bottom of the valence band), we find that $l_{\vec{k}}' \gtrsim b$ for $\Gamma \lesssim \frac{1}{3}$ eV. This means that extra-atomic interferences are important mostly for not too deep hole states and/or relatively light materials. In any case, only the first-nearest neighbors (up to second or third) can contribute in practice, their effect being of course larger for more closely packed lattices.

V. CONCLUSION

So, it appears that, in *photon-induced* Auger emission, deep-hole interferences cannot in general be neglected:

(i) If the atomic hole state is (quasi-) degenerate, there always are intratomic interferences, which have a considerable effect, in particular on the symmetries of angular distributions. They must be taken into account in the numerical calculations used to analyze experimental results.

(ii) For lines corresponding to propagating intermediate states (atomic-V–V or atomic–atomic-V lines), there also are extra-atomic interferences between neighboring atomic sites, provided that the deep-hole level has not too short a lifetime (typically, $\Gamma < 1$ eV). This effect, when present, should be able to give information on the near environment of a given atomic site.

The first problem is of course to check experimentally the importance of extra-atomic interferences. This might be done (apart from including them in numerical calculations of line shapes) by observing the changes of line shapes and angular distributions (AEDC) when the frequency Ω of the incident photon is varied. Indeed, if extra-atomic interferences are absent (due, e.g., to a very large Γ), the EDC and AEDC depend on Ω only via the optical matrix element, which is in general slowly varying in the x-ray range. On the contrary, if extra-atomic interferences are of importance, the EDC and AEDC should change rapidly with Ω, due to rapid oscillation of the primary average spectral density $\bar{\mathcal{C}}_s$. On the other hand, if Ω is such that the primary electrons lie in the far-uv range, their mean free path is so small that it should completely kill extra-atomic effects. Such an experimental situation could thus allow for comparison between a given Auger line with and without extra-atomic effects.

Let us now discuss briefly interferences in the case of *electron-induced* Auger emission. This case can of course be described within the formalism which we have used for photons. The main physical difference is the following: the absorption of monochromatic photons by an electron in a narrow deep state results in primary electrons of well-defined energy $\epsilon_s = \epsilon_h + \Omega$. The scattering of monocinetic electrons of energy Ω by an electron in the same deep state gives rise to *pairs* of electrons of wave vectors $\vec{s}_1, \vec{s}_2$, of which only the total energy $\epsilon_{\vec{s}_1} + \epsilon_{\vec{s}_2} = \epsilon_h + \Omega$ is fixed. The phase factor in the Auger current associated with each Coulomb scattering process giving rise to deep-hole creation is $\exp[i(\vec{s}_1 + \vec{s}_2)\cdot\vec{R}_{\lambda\lambda'}]$ [which replaces the optical phase factor $\exp(i\vec{s}\cdot\vec{R}_{\lambda\lambda'})$]. One must sum the contributions of all energy-conserving $(\vec{s}_1, \vec{s}_2)$ processes. As is known for example from electron energy-loss experiments, for $\epsilon_h + \Omega$ in the keV range, ϵ_{s_1} and ϵ_{s_2} are spread on a width $\gtrsim$ $\gtrsim 100$ eV. This considerable "line width" results in a washing out of the Auger phase coherence on a distance smaller than the atomic length, and therefore kills extra-atomic interferences. On the contrary, intra-atomic interferences $(\vec{R}_{\lambda\lambda'} = 0)$ are not affected since, as in the photon case, two holes on the same atomic site always have perfect phase coherence.

One therefore expects differences between photon- and electron-induced Auger atomic-V-V lines and angular distributions corresponding to relatively narrow hole levels, ascribable to the presence or absence of extra-atomic deep-hole interferences. A systematic study of these differences can be used to get an experimental check of the importance of these effects.

ACKNOWLEDGMENTS

It is a pleasure to thank J. P Briand, R. M. Hochstrasser, M. Hulin, and P. Nozieres for fruitful discussions on this and related topics.

*Supported by a doctoral grant of the Consejo Nacional de Ciencia y Tecnologia de México and by the Centro de Investigacion del Instituto Politecnico Nacional de México.

†Also at Départment de Physique, UER de Sciences Exactes et Naturelles, Université de Picardie, 33 rue Saint-Leu–80000 Amiens, France.

[1]D. Chattarji, *The Theory of Auger Transitions* (Academic, New York, 1976).

[2]J. T. Yue and S. Doniach, Phys. Rev. B 8, 4578 (1973).

[3]P. Noziéres and E. Abrahams, Phys. Rev. B 10, 3099 (1974).

[4]C. Caroli, D. Lederer-Rozenblatt, B. Roulet, and D. Saint-James, Phys. Rev. B 8, 4552 (1973).

[5]P. J. Feibelman and D. E. Eastman, Phys. Rev. B 10, 4932 (1974).

[6]L. V. Kjeldysh, Sov. Phys.-JETP 20, 1018 (1965).

[7]P. H. Citrin, J. E. Rowe, and S. B. Christman, Phys. B 14, 2642 (1976).

[8]G. F. Amelio, Surf. Sci. 22, 301 (1970).

[9]C. D. Graham, Met. Progr. 71, 75 (1957).

[10]L. M. Roth, thesis (Harvard University, 1957) (unpublished).

[11]In a description in terms of atomic wave functions, this limits the deep-hole sites to the extraction depth, but if intersite effects are present, sites μ [see Eq. (23)] can extend to a layer of depth $l_\omega \cos\theta + D$, where D is the range of intersite interactions.